Research on Image Segmentation of Complex Environment Based on Variational Level Set

Hang Li, Dan Li(✉), Kailiang Zhang, and Chuangeng Tian

Xuzhou University of Technology, Xuzhou 221000, Jiangsu, China

Abstract. An improved image segmentation model was established to achieve accurate detection of target contours under high noise, low resolution, and uneven illumination environments. The new model is based on the variational level set algorithm, which improves the C-V (Chan and Vese) model, fuses the contour and area models to segment the image information, and solves the problem of optimal solution of the energy model by finding the steady-state solution of the partial differential equation. It can improve the calculation accuracy, topological structure adaptability, anti-noise ability, and reduce the light sensitivity effectively. Experiment shows that the new model has good robustness, high real-time performance, and it can effectively improve detection accuracy.

Keywords: Variational level set · Contour model · Image segmentation · C-V model

1 Introduction

In recent years, active contour models have received widespread attention in the fields of machine vision and image segmentation [1–3]. Active contour models include parametric active contours and geometric active contour models [4–6]. The parametric Snake active contour model is a commonly used active image segmentation contour model, but the Snake active contour model is sensitive to noise [7–9], it cannot adaptively change the evolution curve topology structure, and requires the segmentation object to be a closed curve, which will not break during segmentation [10–13]. Therefore, the Snake model is not applicable when detecting scattered targets. With the attenuation of the signal in the long-distance network transmission, the image noise will be increased, the resolution will be reduced, and the accurate detection of the target contour will be affected [14, 15]. Therefore, a robust image segmentation algorithm that is not easily disturbed by noise is needed [16–19]. The variational level set geometric active contour model method is a hot topic for scholars due to its topological self-adaptation ability and model integration ability. The method minimizes the energy function, and obtains the PDE (Partial Differential Equation) [20, 21] partial differential equation of level set evolution [22, 23]. By adding constraint information in the energy function, the image has good topological adaptability during segmentation. Li and his team proposed a level set-based ICP model, which used gray-scale clustering to segment images [24], but there will be

© ICST Institute for Computer Sciences, Social Informatics and Telecommunications Engineering 2021
Published by Springer Nature Switzerland AG 2021. All Rights Reserved
H. Song and D. Jiang (Eds.): SIMUtools 2020, LNICST 370, pp. 691–701, 2021.
https://doi.org/10.1007/978-3-030-72795-6_55

over-segmentation problems for weak-boundary images. The C-V model based on region information proposed by Chan and his team is a non-linear image processing method, which can segment images without obvious texture features, discrete distribution, blurred borders, but it has poor anti-light sensitivity [25].

High noise, uneven illumination, image signal attenuation and low resolution are widely existed in complex environment [26–30]. It is not ideal to use the existing model directly. In this paper, geometric active contour model was studied, the C-V model based on the variational level set was improved, and a new model which fused edge and area information was proposed. The new model combines contour and area models to segment image information. By finding steady-state solutions to partial differential equations, it can better solve the problems of obtaining optimal solutions for energy models, have certain topological structure adaptability and anti-light sensitivity.

2 Variational Level Set Method

The active contour model expresses the deformation of curves and surfaces in the form of parametric curves and surfaces [31, 32]. The active contour model expresses the deformation of curves and surfaces in the form of parametric curves and surfaces [33, 34]. Its parameterization is as follows: $\mathbf{v}(s) = (x(s), y(s)), s \in [0, 1]$, where s is the curve parameter, x, y is the coordinate of the contour point. The expression of total energy of dynamic contour is as follows:

$$E_{snake} = \int_0^1 E_{snake}(\mathrm{v}(s))ds = \int_0^1 E_{int}(\mathrm{v}(s)) + E_{ext}(\mathrm{v}(s))ds \tag{1}$$

E_{int} represents the internal energy generated by curve bending, which makes the model smooth and continuous. E_{ext} represents the external energy of the image, which comes from external constraints or image features and attracts the contour to the image feature location. Under the joint action of internal and external energy, the curve converges to the target boundary and has the minimum energy.

Since Snake's active contour model is an edge-based algorithm, it requires the target to be a closed curve, so no segmentation problems will occur when using it for segmentation. In order to detect multiple targets, the level set method was used in this paper.

2.1 Level Set Method

A closed plane curve can be defined as the level set u(x,y) of a two-dimensional function: $\mathrm{C} = \{(\mathrm{x,y}), u(\mathrm{x,y}) = c\}$.

If C changes, then it can be considered that the u(x,y) changes. A closed curve over time can be expressed as a level set changing with time.

$$\mathrm{C(t)} := \{(\mathrm{x,y}), u(\mathrm{x,y,t}) = c\} \tag{2}$$

When the curve C(t) is evolving, the evolution of the embedded function u(x,y,t) follows the following rules:

Total derivative $\frac{du}{dt} = \frac{\partial u}{\partial t} + \nabla u \cdot \frac{\partial (x,y)}{\partial t} = 0$, due to $\frac{\partial (x,y)}{\partial t} = \frac{\partial C}{\partial t} = V$, so

$$\frac{\partial u}{\partial t} = -\nabla u \cdot V = -|\nabla u| \frac{\nabla u}{|\nabla u|} \cdot V = |\nabla u| N \cdot V = \beta |\nabla u| \tag{3}$$

Where $\beta = V \cdot N$ represents the motion velocity normal vector. The above formula is the basic evolution equation of horizontal set curve.

If u (x,y) > c, (x,y) is outside the closed curve C.

If u (x,y) < c, (x,y) is inside closed curve C.

If u(x,y) = c, (x,y) is on closed curve C.

For convenience, c = 0 is often taken, which is the zero level set of the curve. The evolution of the closed curve C is the evolution of the embedded function which is given the initial value u_0(x,y). As long as the level set of u(x,y) = 0 is obtained at time t, the curve C(t) can be determined.

The evolution process is a curve-oriented evolution of a two-dimensional function in space u(x,y,t).The level set method is a no-argument method, the partial differential equations of which are given in a fixed coordinate system. In the process of curve evolution, there is no need to track topological changes because the changes in topology will be automatically embedded in the numerical changes of u(x,y,t).

2.2 C-V Variational Level Set Model

T.Chan and L.Vese proposed the C-V model, it was also known as the geodesic active area model [35, 36], which can be distinguished by the average gray level of the inner and outer regions of the image [37, 38]. The following energy function was proposed:

$$E(c_1, c_2, C) = \mu \oint_C ds + \lambda_1 \iint_{\Omega_1} (I - c_1)^2 dxdy + \lambda_2 \iint_{\Omega_2} (I - c_2)^2 dxdy \tag{4}$$

In the above formula, c_1 and c_2 are scalars, C represents the curve, the first term represents the full arc length of the curve C, the second term represents the square error between the gray value of the internal area and c_1, and the third term represents the square error between the gray value of the external area and c_2. Only when C is in the correct position, two and three terms can reach the minimum at the same time.

The Heaviside function is introduced in the above formula, and the variational level set method is used to modify the functional of the embedded function u:

$$E(c_1, c_2, u) = \mu \iint_{\Omega} \delta(u) |\nabla u| dxdy + \lambda_1 \iint_{\Omega} (I - c_1)^2 H(u) dxdy + \lambda_2 \iint_{\Omega} (I - c_2)^2 (1 - H(u)) dxdy \tag{5}$$

If u is fixed, the above formula can be minimized relative to c_1 and c_2, and we can get the follow formula:

$$c_j = \frac{\iint_{\Omega_j} I dxdy}{\iint_{\Omega_j} dxdy} \; j = 1, 2 \tag{6}$$

c_1 is the average value of the input image I inside the curve, and c_2 is the average value of the image I outside the curve. When c_1 and c_2 are fixed, the relative minimization can be obtained as the following formula. A steady state solution of the segmentation results can be obtained by simultaneous.

$$\frac{\partial \mathrm{u}}{\partial t} = \delta_\varepsilon \left[\mu div(\frac{\nabla u}{|\nabla u|}) - \lambda_1 (I - c_1)^2 + \lambda_2 (I - c_2)^2 \right] \tag{7}$$

Figure 1 is a gray image with size of 100 * 100 pixels which iterated under the common and the lighting conditions, respectively. In Fig. 1-a, from the left to the right, the images were iterated 0, 30, 40 and 50 times. The convergence speed is fast and the effect is good. The round holes inside the tool can also be accurately detected. In Fig. 1-b, from the left to the right, the images were iterated 0, 50, 100 and 200 times. Due to the effects of light, the C-V model was affected by light, it converged slowly, and finally failed the segmentation.

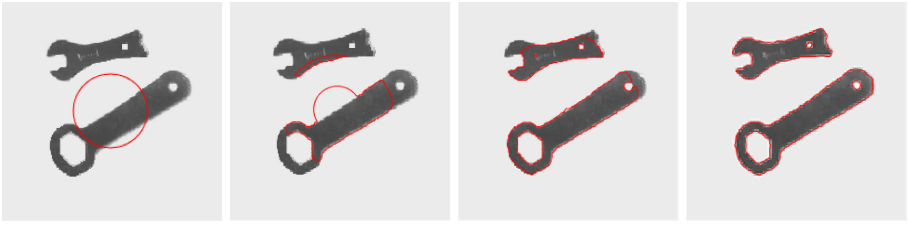

(a)Segmentation in common environment

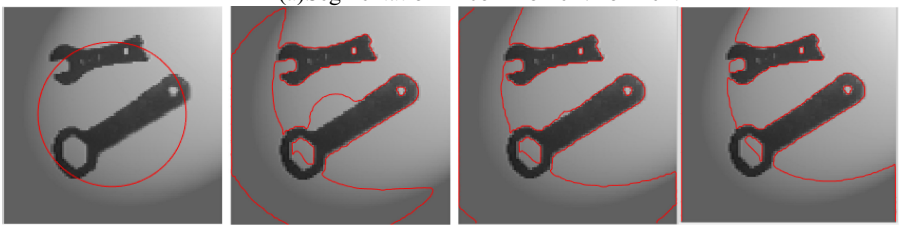

(b) Segmentation in lighting environment

Fig. 1. Segmentation of C-V model in common and uneven lighting environment

Figure 2 is a gray image with size of 152 * 152 pixels. The C-V model segmentation with different initial values was performed separately. The results are as follows:

As shown in Fig. 2, image is segmented under different initial contour conditions for the same noise. The initial contour in the first line is small, and the numbers of iterations are 0, 40, 60, and 80. There is severe noise interference in the background, but it still converges quickly to the edges. The initial contour of the second image is large, and the numbers of iterations are 0, 50, 100 and 300. Although the number of iterations is higher and the speed is slower than the first line, the final segmentation effect is still very accurate. At 300 frames, it converges completely with the boundary.

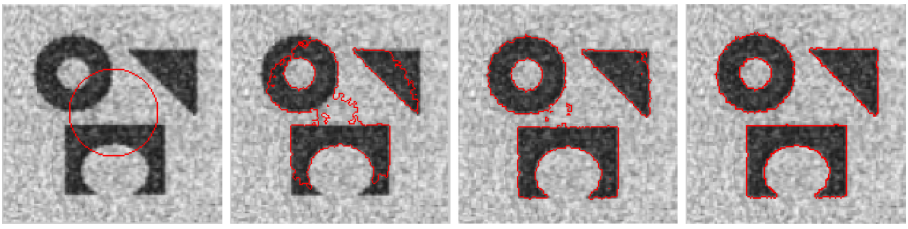

(a) Small initial contour

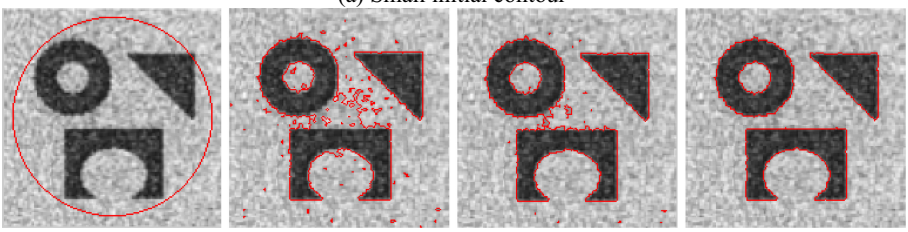

(b)Large initial contour

Fig. 2. Segmentation of C-V model in noisy environment

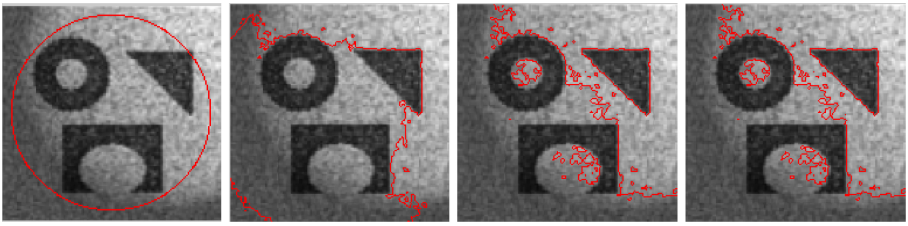

Fig. 3. Segmentation of C-V model in noisy and uneven lighting environments

Figure 3 is C-V model segmentation under noisy and uneven lighting environment, The algorithm is very easily interfered by illuminance. The figure shows the results of iterations of 0, 10, 50, and 300 times. It is easy to fall into local extremes and cannot effectively segment the target.

3 Improved Image Segmentation Model

The above experiments show that the C-V model uses the global information of the homogeneous region of the image to effectively improve the ability of adaptive adjustment of the curve topology [39, 40]. In the segmentation process, the image boundary is not required to be clear, and it has good noise immunity. However, it does not consider the inherent characteristics of the level set function, and does not use the target boundary information. Therefore, the edge positioning is not accurate, and it is extremely sensitive to light. Based on the research, this paper proposes a new method to improve the C-V model for the environment with noisy and uneven illumination. The new model combines the boundary-based segmentation method with the region-based segmentation method, which can be relatively complemented.

Combining the C-V model and the edge information, the following energy functional is obtained:

$$\begin{aligned} E(c_1, c_2, C) &= E_{GAC}(C) + E_{C-V}(c_1, c_2, C) \\ &= \mu \oint_C g ds + \lambda_1 \iint_{\Omega_1} (I - c_1)^2 dxdy + \lambda_2 \iint_{\Omega_2} (I - c_2)^2 dxdy \end{aligned} \tag{8}$$

The introduction of the edge function g enhances the accuracy of edge extraction. Rewrite the above functional with the variational level set:

$$E(c_1, c_2, u) = \mu \iint_{\Omega} \delta(u) g |\nabla u| dxdy + \lambda_1 \iint_{\Omega} (I - c_1)^2 H(u) dxdy + \lambda_2 \iint_{\Omega} (I - c_2)^2 (1 - H(u)) dxdy \tag{9}$$

For the formula (10):

$$E(u) = \iint_{\Omega} g(x, y) \delta(u) |\nabla u| dxdy \tag{10}$$

The paper improves the above formula. Adding a diffusion term in the energy functional to keep the embedded function as a distance function, it can be transformed into:

$$E(u) = \mu \iint_{\Omega} \frac{1}{2} (|\nabla u| - 1)^2 dxdy + \iint_{\Omega} g(x, y) \delta(u) |\nabla u| dxdy \tag{11}$$

Where u is the constant. The improved variational level set model can make the embedding function $u_0(x, y)$ approximate to the distance function, the work of initializing the embedding function can be greatly simplified, and re-initialization can be completely avoided.

When u is fixed and minimized relative to c_1, c_2, and the following partial differential equation is obtained:

$$\frac{\partial \mathrm{u}}{\partial t} = \mu_1 \left[\Delta u - div(\frac{\nabla u}{|\nabla u|}) \right] + \delta_\varepsilon \left[\mu_2 div(g \frac{\nabla u}{|\nabla u|}) - \sum_{i=1}^{m} \lambda_{1i} (I - c_{1i})^2 + \sum_{i=1}^{m} \lambda_{2i} (I - c_{2i})^2 \right] \tag{12}$$

The discretization of Δu adopts 4-neighbor difference scheme.

$$(\Delta u)_{i,j} = u_{i+1,j} + u_{i-1,j} + u_{i,j+1} + u_{i,j-1} - 4u_{i,j} \tag{13}$$

The magnitude of the effect of the forced term is controlled by μ. In the case of $\tau\mu \leq 0.25$, the gradient descent flow explicit scheme is stable, and $\tau \approx 0.1, \mu \approx 2$ can be taken. Discrete operators need to be discretized. The "half-point discretization" scheme can be used.

$$div(\frac{\nabla u}{|\nabla u|}) = \frac{\partial}{\partial x}(g \frac{u_x}{|\nabla u|}) + \frac{\partial}{\partial y}(g \frac{u_y}{|\nabla u|}) \tag{14}$$

From the above formula, the following formula can be obtained.

$$div(g\frac{u}{|\nabla u|}) \approx g_{i,j+1/2}(\frac{u_x}{|\nabla u|})_{i,j+1/2} - g_{i,j-1/2}(\frac{u_x}{|\nabla u|})_{i,j-1/2} + g_{i+1/2,j}(\frac{u_y}{|\nabla u|})_{i+1/2,j} - g_{i-1/2,j}(\frac{u_y}{|\nabla u|})_{i-1/2,j} \tag{15}$$

Express each term in the above formula with the values of u and g at the Integer value. For example, in the first item of formula (15):

$$(\nabla u)_{i,j+1/2} = ((u_x)_{i,j+1/2}, (u_y)_{i,j+1/2}) \tag{16}$$

$$(u_x)_{i,j+1/2} = u_{i,j+1} - u_{i,j} \tag{17}$$

$$(u_y)_{i,j+1/2} = (u_{i+1,j+1/2} - u_{i-1,j-1/2})/2 = (u_{i+1,j+1} + u_{i+1,j} - u_{i-1,j+1} - u_{i-1,j})/4 \tag{18}$$

Therefore, the following formula can be got.

$$(\frac{u_x}{|\nabla u|})_{i,j+1/2} = (u_x)_{i,j+1/2}/\sqrt{(\nabla u)^2_{i,j+1/2} + (u_y)_{i,j+1/2}}$$
$$= (u_{i,j+1} - u_{i,j})/[(u_{i,j+1} - u_{i,j})^2 + (u_{i+1,j+1} + u_{i+1,j} - u_{i-1,j+1} - u_{i-1,j})^2/16]^{1/2} \tag{19}$$

$$= C_{1,i,j}(u_{i,j+1}, u_{i,j})$$
$$C_{1,i,j} = 1/(u_{i,j+1} - u_{i,j})^2 + (u_{i+1,j+1} + u_{i+1,j} - u_{i-1,j+1} - u_{i-1,j})^2/16]^{1/2} \tag{20}$$

The value of g at half point can be approximated by the average of two adjacent points:

$$g_{i+1/2,j} = (g_{i+1,j} + g_{i,j})/2 \tag{21}$$

The other three items are also processed like above formulas to get the formula (15). Then the upwind scheme can be used for calculations.

$$div(g\frac{\nabla u}{|\nabla u|})_{i,j} \approx C_{1,i,j}g_{1,i,j}(u_{i,j+1} - u_{i,j}) - C_{2,i,j}g_{2,i,j}(u_{i,j} - u_{i,j-1}) + C_{3,i,j}g_{3,i,j}(u_{i+1,j} - u_{i,j}) - C_{4,i,j}g_{4,i,j}(u_{i,j} - u_{i-1,j}) \tag{22}$$

4 Experiment and Analysis

The experimental environment includes Windows 10 operating system, 8G memory, 3.6 GHZ CPU, and MATLAB 2018. In Fig. 4, (b) is the result of the improved model in the common environment for coin image segmentation. The numbers of iterations are 0, 15, 30 and 50 times respectively. (b) is the result of the improved model in the

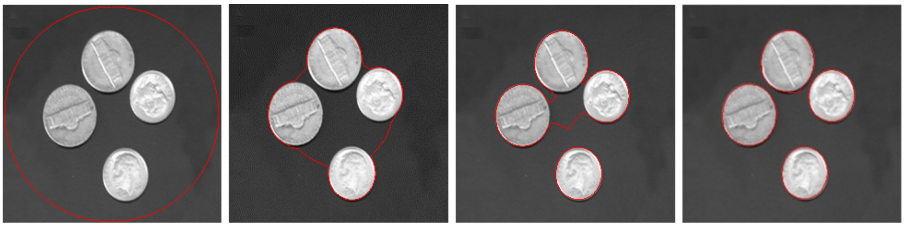

(a)Segmentation of coins in common environment

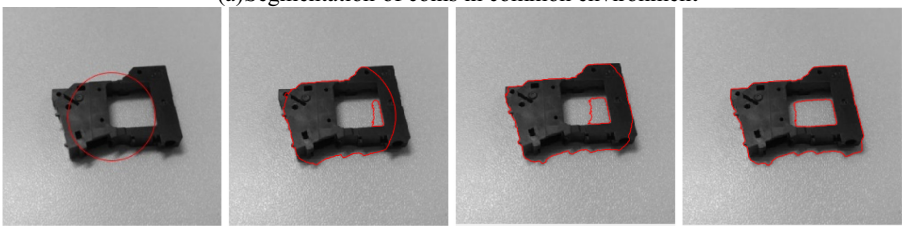

(b)Segmentation of part in low noisy environment

Fig. 4. Segmentation of improved model in common and low noisy environments

Table 1. Number and time of iterations in improved models

Images	Number of iterations	Time (seconds)
(a)	15	0.419718
	30	0.749150
	50	1.170998
(b)	20	0.736783
	40	1.339194
	60	1.727235

low noise environment. The numbers of iterations are 0, 20, 40, 60 times respectively. The starting position in figure (b) is different from figure(a). The improved algorithm has better shrinkage effect no matter it shrinks inward or expands outward, and it can effectively detect the empty area in figure (b). The time consumption in Fig. 4 is shown in Table 1.

The high-noise image and the uneven illumination image are segmented by the new method in Fig. 5.

In Fig. 5, it can be seen that the new model implemented by improving the variational level set has better convergence results for the problems that the above C-V model cannot solve. It has fast convergence speed and good robustness in complex environments such as low contrast, noisy, and blur. During the shrinking process, not only the outer boundary of the target is detected clearly, but also the inner boundary, whether it is concave or hollow, can be detected well. The improved new model has a good effect on the contour

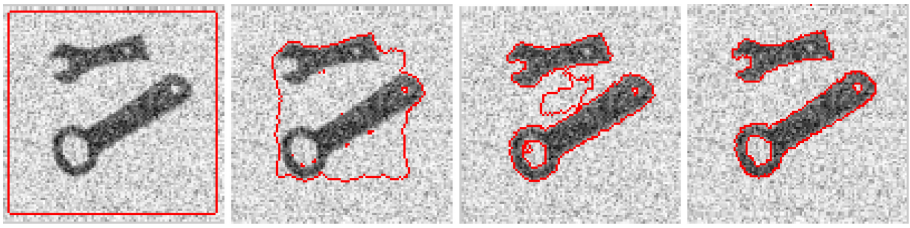

(a)Segmentation in noisy environment

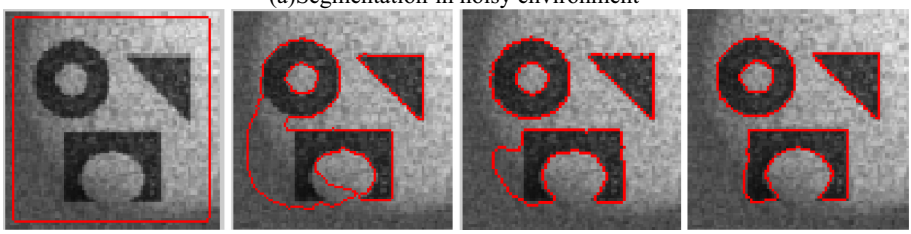

(b)Segmentation in noisy and uneven lighting environment

Fig. 5. Segmentation of improved model in noisy and uneven lighting environments

detection of multiple targets. The results show that the new model proposed in this paper is more accurate than C-V model segmentation and has better ability to resist complex environments.

5 Conclusion

This paper analyzes and studies the image segmentation model based on variational level set. Aiming at the complex environment of uneven illumination, blurred video image and noisy environment, this paper proposes an improved model that combines edge and area information. State solution, the optimal solution of the energy model is obtained, and the numerical calculation is performed by using a half-point discretization difference scheme, thereby improving the calculation accuracy. Experiments show that compared with other models, the complex environment segmentation model established in this paper has more accurate segmentation and high real-time performance. It solves the problems of illumination, noise sensitivity and inaccurate edge positioning of the original model.

Acknowledgement. This work is partly supported by the Science and Technology Project of Jiangsu Provincial Department of Housing and Construction (2019ZD039), Major Projects of Natural Science Research in Universities of Jiangsu Province (19KJA470002).

References

1. Zhou, S., Kan, P., Silbernagel, J., Jin, J.: Application of image segmentation in surface water extraction of freshwater lakes using radar data. ISPRS Int. J. Geo-Inf. **9**(7), 424 (2020)
2. Zhang, Y., Chen, P., Hong, H., Huang, Z., Zhou, C.: The research of image segmentation methods for interested area extraction in image matching guidance. In: MIPPR 2019: Automatic Target Recognition and Navigation, Vol. 11429, p. 114290R International Society for Optics and Photonics (2020)
3. Sakaridis, C., Dai, D., Van Gool, L.: Map-guided curriculum domain adaptation and uncertainty-aware evaluation for semantic nighttime image segmentation. arXiv preprint arXiv:2005.14553 (2020)
4. Xia, G.S., Liu, G., Yang, W., Zhang, L.P.: Meaningful object segmentation from sar images via a multiscale nonlocal active contour model. IEEE Trans. Geosci. Remote Sens. **54**(3), 1860–1873 (2016)
5. Li, H., Gong, M.G., Liu, J.: A local statistical fuzzy active contour model for change detection. IEEE Trans. Geosci. Remote Sens. **12**(3), 582–586 (2015)
6. Jiang, D., Huo, L., Li, Y.: Fine-granularity inference and estimations to network traffic for SDN. PLoS ONE **13**(5), 1–23 (2018)
7. Jiang, D., Zhang, P., Lv, Z., et al.: Energy-efficient multi-constraint routing algorithm with load balancing for smart city applications. IEEE Internet Things J. **3**(6), 1437–1447 (2016)
8. Yu, S., Lu, Y., Molloy, D.: A dynamic-shape-prior guided snake model with application in visually tracking dense cell populations. IEEE Trans. Image Process. **28**(3), 1513–1527 (2019)
9. Jiang, D., Li, W., Lv, H.: An energy-efficient cooperative multicast routing in multi-hop wireless networks for smart medical applications. Neurocomputing **220**(12), 160–169 (2017)
10. Ren, H., Su, Z.B., Lv, C.H., Zou, F.J.: An improved algorithm for active contour extraction based on greedy snake. In: IEEE/ACIS 14th International Conference on Computer and Information Science (ICIS), pp. 589-592 (2015) https://doi.org/10.1109/ICIS.2015.7166662
11. Celestine, A., Peter, J.D.: Investigations on adaptive connectivity and shape prior based fuzzy graph-cut colour image segmentation. Expert Syst. **37**(5), e12554 (2020)
12. Feng, C., Yang, J., Lou, C., Li, W., Zhao, D.: A global inhomogeneous intensity clustering-(GINC-) based active contour model for image segmentation and bias correction. Comput. Math. Methods Med. **2020**(5), 1–8 (2020)
13. Wang, Y., Jiang, D., Huo, L., Zhao, Y.: A new traffic prediction algorithm to software defined networking. Mob. Netw. Appl. pp. 1-10 (2019)
14. Jiang, D., Wang, Y., Lv, Z., Wang, W., Wang, H.: An energy-efficient networking approach in cloud services for IIoT networks. IEEE J. Sel. Areas Commun. **38**(5), 928–941 (2020)
15. Huo, L., et al.: An intelligent optimization-based traffic information acquirement approach to software-defined networking. Comput. Intell. **36**(1), 151-171 (2019)
16. Arbeláez, P., Maire, M., Fowlkes, C., Malik, J.: Contour detection and hierarchical image segmentation. IEEE Trans. Pattern Anal. Mach. Intell. **33**(5), 898–916 (2011)
17. Mariano, R., Oscar, D., Washington, M., Alonso, R.M.: Spatial sampling for image segmentation. Comput. J. **55**(3), 313–324 (2018)
18. Jiang, D., Wang, Y., Lv, Z., Qi, S., Singh, S.: Big data analysis based network behavior insight of cellular networks for industry 4.0 applications. IEEE Trans. Ind. Inform. **16**(2), 1310–1320 (2020)
19. Huo, L., et al.: An AI-based adaptive cognitive modeling and measure-ment method of network traffic for EIS. Mob. Netw. Appl. 1-11 (2019)
20. Avalos, G., Geredeli, P.G.: Exponential stability of a non-dissipative, compressible flow–structure PDE model. J. Evol. Eqn. **20**(1), 1–38 (2020)

21. Xia, M., Greenman, C.D., Chou, T.: PDE models of adder mechanisms in cellular proliferation. SIAM J. Appl. Math. **80**(3), 1307–1335 (2020)
22. Kolářová, E., Brančík, L.: Noise influenced transmission line model via partial stochastic differential equations. In: 2019 42nd International Conference on Telecommunications and Signal Processing (TSP), pp. 492-495. IEEE (2019). https://doi.org/10.1109/TSP.2019.8769101
23. Pels, A., Gyselinck, J., Sabariego, R.V., Schops, S.: Solving nonlinear circuits with pulsed excitation by multirate partial differential equations. IEEE Trans. Magn. **54**(3), 1–4 (2017)
24. Li, C., Huang, R., Ding, Z., Gatenby, J.C.: A level set method for image segmentation in the presence of intensity inhomogeneities with application to MRI. IEEE Trans. Image Process. **20**(7), 2007–2015 (2011)
25. Chan, T.F., Vese, L.A.: Active contours without edges. IEEE Trans. Image Process. **10**(2), 266–277 (2001)
26. Jiang, D., Huo, L., Song, H.: Rethinking behaviors and activities of base stations in mobile cellular networks based on big data analysis. IEEE Trans. Netw. Sci. Eng. **7**(1), 80–90 (2020)
27. Qi, S., Jiang, D., Huo, L.: A prediction approach to end-to-end traffic in space information networks, Mob. Netw. Appl. pp. 1-10 (2019)
28. Jiang, D., Wang, W., Shi, L., Song, H.: A compressive sensing-based approach to end-to-end network traffic reconstruction. IEEE Trans. Netw. Sci. Eng. **7**(1), 507–519 (2020)
29. Jiang, D., Huo, L., Lv, Z., Song, H., Qin, W.: A joint multi-criteria utility-based network selection approach for vehicle-to-infrastructure networking. IEEE Trans. Intell. Transp. Syst. **19**(10), 3305–3319 (2018)
30. Wang, F., Jiang, D., Qi, S.: An adaptive routing algorithm for integrated information networks. China Commun. **7**(1), 196–207 (2019)
31. Li, D., Tian, J., Xiao, L.Q., Sun, J.P., Cheng, D.Q.: Target tracking method based on active contour models combined camshift algorithm. Video Eng. **39**(19), 101–104 (2015)
32. Liu, G., Dong, Y., Deng, M., Liu, Y.: Magnetostatic active contour model with classification method of sparse representation. J. Electr. Comput. Eng. **2020**(9), 1–10 (2020)
33. Zhang, H., Wang, G., Li, Y., Wang, H.: Faster r-cnn, fourth-order partial differential equation and global-local active contour model (FPDE-GLACM) for plaque segmentation in IV-OCT image. SIViP **14**(3), 509–517 (2020)
34. Ali, H., Sher, A., Saeed, M., Rada, L.: Active contour image segmentation model with de-hazing constraints. IET Image Proc. **14**(5), 921–928 (2020)
35. Xiao, J.S., et al.: The improvement of C-V level set method for image segmentation. In: International Conference on Computer Science and Software Engineering, pp. 1106–1109 (2008)
36. Tan, H.Q., et al.: C-V level set based cell image segmentation using color filter and morphology. In: International Conference on Information Science, Electronics and Electrical Engineering, Vol. 2, pp. 1073-1077. IEEE (2014). https://doi.org/10.1109/InfoSEEE.2014.6947834
37. Yu, S., Yiquan, W.: A morphological approach to piecewise constant active contour model incorporated with the geodesic edge term. Mach. Vis. Appl. **31**(4), 1–25 (2020). https://doi.org/10.1007/s00138-020-01083-4
38. Sarotte, C., Marzat, J., Piet-Lahanier, H., Ordonneau, G., Galeotta, M.: Model-based active fault-tolerant control for a cryogenic combustion test bench. Acta Astronautica **177**, 457-477 (2020)
39. Kai, L.I., Jianhua, Z., Shuqing, H., Fantao, K., Jianzhai, W.U.: Target extraction of cotton disease leaf images based on improved C-V model. J. China Agric. Univ. (2019)
40. Lakra, M., Kumar, S.: A CNN-based computational algorithm for nonlinear image diffusion problem. Multimedia Tool Appl. **79**(33), 23887-23908 (2020)